

Journal of Materials Chemistry B

Accepted Manuscript



This is an *Accepted Manuscript*, which has been through the Royal Society of Chemistry peer review process and has been accepted for publication.

Accepted Manuscripts are published online shortly after acceptance, before technical editing, formatting and proof reading. Using this free service, authors can make their results available to the community, in citable form, before we publish the edited article. We will replace this *Accepted Manuscript* with the edited and formatted *Advance Article* as soon as it is available.

You can find more information about *Accepted Manuscripts* in the [Information for Authors](#).

Please note that technical editing may introduce minor changes to the text and/or graphics, which may alter content. The journal's standard [Terms & Conditions](#) and the [Ethical guidelines](#) still apply. In no event shall the Royal Society of Chemistry be held responsible for any errors or omissions in this *Accepted Manuscript* or any consequences arising from the use of any information it contains.

Biocompatible long-circulating star carboxybetaine polymers

Weifeng Lin^a, Guanglong Ma^a, Fangqin Ji^a, Juan Zhang^a, Longgang Wang^a, Haotian Sun^a,
Shengfu Chen^{a,b*}

^a Key Laboratory of Biomass Chemical Engineering of Ministry of Education, Department of
Chemical and Biological Engineering, Zhejiang University, Hangzhou, Zhejiang 310027, China

^b Jiangsu Collaborative Innovation Center of Biomedical Functional Materials, Jiangsu Key
Laboratory of Biomedical Materials, College of Chemistry and Materials Science, Nanjing
Normal University, Nanjing 210046, China

Abstract:

Polyethylene glycol (PEG) is considered as the most effective material to prolong the circulation time of nanoparticles through reducing non-specific protein adsorption in blood. However, it is recognized that PEG decomposes in most physiological solutions; and an anti-PEG antibody has been detected in some normal blood donors as a response to injection with PEGylated polymer particles. Zwitterionic polymers are potential alternatives to PEG for biomedical applications due to their super resistance to non-specific protein adsorption. Thus, finding one polymer processing long circulation time and resisting immune response is of great importance. Here, we prepared four star carboxybetaine polymers of different molecular weights via atom transfer radical polymerization (ATRP) from a β -cyclodextrin (β -CD) initiator for investigating the biocompatibility of carboxybetaine polymer, a typical zwitterionic polymer. The circulation half-life of the largest star polymer (123 kDa) in mice was prolonged to 40 h in vivo, with no appreciable damage or inflammation observed in major organ tissues. Furthermore, the circulation time of repeat injections showed similar results to the first injection, with no obvious increase of antibody amount occurred in blood. The internalization of the star carboxybetaine polymers by macrophage cell was a relatively slow process. The cell viability in presence of star carboxybetaine polymers is up to 2 mg/mL. The hemolytic activity of the star carboxybetaine polymers at 5 mg/mL was almost undetectable. *In vitro* results prove a key prediction of excellent biocompatibility in vivo. All the results suggest that the carboxybetaine polymer, perhaps most of the zwitterionic ones, might be a good alternative to PEG in the development of drug

1 delivery system.

2 **Key words:** star carboxybetaine polymers; long-circulating; repeated injection;

3 * **To whom correspondence should be addressed:** E-mail: schen@zju.edu.cn.

4

5 **1. Introduction**

6 Non-ionic polyethylene glycol (PEG)¹ and oligo(ethylene glycol) (OEG)², which
7 exhibit both hydrophilic and amphiphilic characteristics, are the most commonly used
8 stealth materials. However, it has been recognized that PEG and OEG decompose in
9 the presence of oxygen and transition metal ions found in most biochemically relevant
10 solutions for long-term application.³ Furthermore, PEG antibodies occur in animals
11 and even humans, which may lead to strongly reduced bio-availability of a PEGylated
12 drug or even cause undesirable pathological side effects.^{4,5} A possible interaction of
13 PEG with biological macromolecules suggests a possible mechanism of PEG
14 protection might be involved due to the amphiphilic nature of PEG.^{6,7} Unlike
15 amphiphilic PEG, zwitterionic polymers, such as poly(2-methacryloyloxyethyl
16 phosphorylcholine) (pMPC)⁸⁻¹⁰, poly(sulfobetaine methacrylate) (pSBMA)¹¹⁻¹³,
17 poly(carboxybetaine methacrylate) (pCBMA)¹⁴⁻¹⁶ and simply mixed-charge materials,
18 etc¹⁷⁻¹⁹ are super-hydrophilic via electrostatic interaction with water and have been
19 recognized as effective nonfouling materials which can resist protein adsorption and
20 cell attachment. Polyzwitterionic materials might be a good alternative to PEGs to
21 achieve excellent stability in blood stream. Thus, it is important to illustrate the
22 biocompatibility of zwitterionic polymers both *in vivo* and *in vitro*, especially long
23 circulation time and no immune response of zwitterionic polymers *in vivo*.
24 Meanwhile, more and more experimental results showed the advantages of
25 zwitterionic polymer in biomedical applications.^{20,21} Jiang and coworkers reported
26 good retention of hydrophilic drug and long blood circulating characteristics of
27 pCBMA-modified liposomes without cholesterol shine a light on the superior
28 biocompatibility.²² Moreover, they also prepared poly(lactic-co-glycolic acid)
29 (PLGA)-b-pCBMA block copolymers (PLGA-PCB), and found that their

1 self-assembled nanoparticles were remarkably stable without any
2 cryoprotectant additives after freeze-drying.¹⁴ Recent results reported by Wooley
3 and coworkers indicated a better shielding efficiency provided by PEG than PCB
4 polymers to the immunotoxic nanoparticles.²³ In fact, the biocompatibility of the
5 materials forming nano-drug vehicles (NDVs) plays a decisive role in nano-drug
6 delivery. NDVs administered by the parenteral route could spread to most organs and
7 be uptaken by them, mainly by reticulo-endothelial system. Moreover, NDVs will be
8 repeatedly injected, which might cause immunoresponse-related clearance. Previous
9 reports have shown that anti-PEG antibody was detected in some normal blood
10 donors (22%-25%) as a response to injection with PEGylated polymer particles.
11 Rapid clearance of PEGylated polymer particles has been observed.²¹ Meanwhile,
12 some recent studies have reported that nanoparticles may generate potential harm to
13 the body. Such informational shortages become a big hindrance to expand the
14 biomedical applications of related polymers, especially in nano-drug delivery. It is
15 desired to get systematic information on long circulation time and no immune
16 response of zwitterionic polymers.

17 To investigate the biocompatibility of zwitterionic polymers, four RhB-labeled
18 star polymers of different chain lengths were synthesized via atom transfer radical
19 polymerization (ATRP) from a β -CD initiator (Scheme 1) as reliable nanoparticle
20 models due to their well-defined, chemically stable molecular entities with moderate
21 flexibility in structure and surface functionality.²⁴ In addition, it has been shown that
22 at equivalent areas per molecule, a star polymer will be superior to resist non-specific
23 protein adsorption than linear grafts, which have the potential to provide the
24 pharmacokinetic advantages of delivery systems and increase the possibility of drug
25 targeting. Moreover, their diameters are relatively fixed and stable since branches are
26 covalently bonded.²⁵ In this work, both *in vitro* behaviors, such as cell uptake,
27 cytotoxic and hemolytic activity and *in vivo* behaviors, including blood circulation,
28 serum-biochemistry and histopathological responses of the star zwitterionic polymers
29 were investigated systematically. The objective of the study was to determine whether
30 there was little potential toxicity on cell and tissue level, and whether there was long

1 circulation time and no immune response upon repeated injections of zwitterionic
2 polymer. The results of the biocompatibility of zwitterionic polymers are rather
3 encouraging. The circulation half-life of the largest star polymer (123 kDa) in mice
4 was prolonged to 40 h, with little change between the first and the next two doses. The
5 results illustrate that zwitterionic polymers could be excellent alternatives to PEG for
6 drug delivery system.

7

8 **2. Experimental Methods**

9 **2.1 Materials**

10 β -Cyclodextrin (β -CD, 98%), 3-(4,5-dimethylthiazol-2-yl)-2,5-diphenyl
11 tetrazolium bromide (MTT, 98%), 2-(dimethylamino)ethyl methacrylate (DMAEMA,
12 98%), 2-hydroxyethyl methacrylate (HEMA, 98%), 2-bromoisobutyryl bromide
13 (BIBB, 98%), 4-dimethylaminopyridine (DMAP, 99%), copper(I) bromide (CuBr,
14 99%), *N,N',N',N'',N''*-pentamethyldiethylenetriamine (99%), triethylamine
15 (99.5%), rhodamine B (95%), polypropylene oxide 1000 (PPO 1 K), polyethylene
16 glycol 2000 (PEG 2 K), sodium nitrate (NaNO₃) and all the organic solvents were
17 purchased from Aladdin-reagent (Shanghai). β -propiolactone (98%) and
18 dicyclohexylcarbodiimide (DCC, 99%) were purchased from TCI (Shanghai).
19 Fibrinogen from bovine was purchased from Sigma-Aldrich. β -CD was vacuum-dried
20 at 100 °C overnight before use. Carboxybetaine methacrylate (CBMA) was prepared
21 following the procedures reported previously.¹⁶

22

23 **2.2 Characterization**

24 All ¹H NMR spectra were recorded in CDCl₃ or D₂O using a Bruker
25 ADVANCE2B/400MHz instrument at room temperature. Gel permeation
26 chromatography (GPC) measurements were conducted on a Waters GPC system
27 equipped with Waters Ultrahydrogel columns and a Waters refractive index detector.
28 The molecular weight and molecular weight distributions were calibrated against
29 polyethylene glycol standards with 0.2 mol/L NaNO₃ aqueous solutions as eluent at a

1 flow rate of 0.5 mL/min, and the column temperature was 40 °C. The averages
2 diameters of the star polymers were measured by Zetasizer Nano-ZS (Malvern
3 Instruments), the scattering angle was kept at 173° and the temperature was 37 °C.

4

5 **2.3 Synthesis of β -CD-Based Macroinitiator (CD-BIBB)**

6 β -CD-based macroinitiator was prepared following the procedures reported
7 previously.²⁴ β -CD (4 mmol, vacuum-dried at 100 °C overnight before use) was
8 dissolved in 35 mL of anhydrous 1-methyl-2-pyrrolidione (NMP) at room temperature
9 with stirring and then it was cooled to 0 °C. BIBB (25 mmol) dissolved in anhydrous
10 NMP (15 mL) was added dropwise to the β -CD solution with stirring. The reaction
11 mixture was allowed to warm up to ambient temperature and stirred overnight. The
12 final reaction mixture was precipitated with 400 mL of diethyl ether. The white
13 powder precipitate was collected by filtration. The crude product was purified by
14 suspending it in 200 mL of deionized water at room temperature overnight. The
15 purified β -CD-based macroinitiator was filtered, and dried by lyophilization with a
16 yield of 48%.²⁶

17

18 **2.4 Synthesis of Fluorescent Monomer (RhB-HEMA)**

19 Typically, a solution of dicyclohexylcarbodiimide (20 mmol) and
20 4-dimethylaminopyridine (2 mmol) in 160 mL of methylene dichloride was added
21 dropwise to a solution of rhodamine B (10 mmol) and 2-hydroxyethyl methacrylate
22 (20 mmol) in 40 mL of methylene dichloride (Scheme 2). The reaction mixture was
23 stirred overnight. After removing insoluble salts by suction filtration, the filtrate was
24 concentrated and further purified by chromatography (silica gel, 10%
25 isopropanol/ethyl acetate). After removing all the solvents by rotate evaporation,
26 RhB-HEMA was obtained as a solid (2.7 g, yield: 45%) ¹H NMR (CDCl₃, 400
27 MHz): 8.31, 7.83, 7.76, 7.32, 7.09, 6.93 and 6.81 (m, 10 H, Aromatic protons), 6.60 (s,
28 1H), 6.53 (s, 1H), 4.18 (m, 2H), 4.18 (m, 2H), 3.65 (q, 8H), 1.35 (t, 12 H) (Figure 1a).

29

30 **2.5 Synthesis of Star Carboxybetaine Polymers**

1 A typical polymerization procedure of the CD-g-CBMA star polymers
2 (CD-CBMA2) at [CBMA]/[CD-BIBB] ratio of 300 was carried out as follows:
3 CBMA (2.3 mmol), RhB-HEMA (11 μmol), CD-BIBB (7.5 μmol), and 3 mL of
4 methanol/water (9:1, v/v) was deoxygenated with nitrogen for 30 min before adding
5 Cu(I)Br (0.045 mmol) and PMDETA (0.054 mmol) under nitrogen protection. The
6 reaction mixture was maintained under nitrogen purge for the duration of the
7 polymerization. After 12 h, the reaction mixture was exposed to air to stop
8 polymerization. The polymer was dialyzed against methanol for 3 days using a
9 3500-MW cutoff membrane and against water for another 3 days. The star polymer
10 was lyophilized to afford a rose pink solid. The molecular weight was determined by
11 GPC.

12

13 **2.6 Evaluation the Stability of Star Polymers in Protein Solution**

14 The stability of the star polymers against fetal bovine serum (FBS) solution in PBS
15 (pH 7.4, 0.15 M) was investigated using dynamic light scattering (DLS). 1 mL of star
16 polymer (10 mg/mL) prepared in PBS was mixed with 1 mL of fetal bovine serum
17 (FBS) solution (100%) at 37 °C. At 0.5 h, 1 h and 2 h, the size of the star polymer was
18 measured. PPO 1 kDa and PEG 2 kDa were selected as the positive and negative
19 controls.

20

21 **2.7 *In Vitro* Cell Uptake**

22 To study the cellular uptake of the star carboxybetaine polymers by fluorescence
23 microscopy and flow cytometry, RAW 264.7 cells were seeded in 24-well plates
24 supplemented with Dulbecco's modified eagle's medium (DMEM) and 10% fetal
25 bovine serum (FBS) under 5% CO₂ at 37 °C for 24 h. Culture medium was removed
26 and 1.0 mL of RhB-HEMA labeled polymer (0.5 mg/mL) or equivalent RhB-HEMA
27 was added into each well. After 12 h incubation, the cells were rinsed 3 times with
28 PBS and placed in 0.2 mL of DMEM for live cell imaging. Thereafter, the cells were
29 rinsed 3 times with PBS and treated with trypsin. The cells were then suspended in
30 PBS and analyzed immediately using a flow cytometer (BD FACSEALIBURTM).

1

2 **2.8 Hemolysis Assay**

3 The hemolysis assay was performed according to a previous report.²⁷ Fresh
4 blood was collected from healthy male ICR mice. Red blood cells (RBCs) were
5 separated by centrifugation of whole blood diluted in sterile phosphate-buffered
6 saline (PBS) at 1500 rpm for 10 min. The plasma supernatant was removed and the
7 erythrocytes were resuspended in sterile PBS. The cells were washed three times with
8 sterile PBS solution, and then resuspended in PBS to get a 2% w/v RBCs suspension.
9 Star carboxybetaine polymer solutions of different molecular weight were also
10 prepared in sterile PBS. A 0.5 mL of polymer solution prepared in PBS was added to
11 0.5 mL of 2% w/v RBCs suspension to make the final polymer concentration at 5
12 mg/mL and it was incubated for 6 h at 37 °C. After incubation, the mixture was
13 centrifuged and the supernatant was transferred to a 96-well plate. Release of
14 hemoglobin was determined by spectrophotometric analysis of the supernatant at 575
15 nm. Complete hemolysis was attained using double distilled water as positive control
16 and PBS as negative control.

17

18 **2.9 In Vitro Cytotoxic Assay**

19 The cytotoxic effect of star carboxybetaine polymers was determined by using
20 MTT assay. RAW 264.7 or HUVEC cells were seeded (1×10^4 cell/well) in 96-well
21 plates supplemented with Dulbecco's modified eagle medium (DMEM) and 10% fetal
22 bovine serum (FBS) under 5% CO₂ at 37 °C for 24 h. For each well, cells were
23 washed with PBS and incubated with 200 μL full medium containing varied
24 concentration of star carboxybetaine polymers for 24 h. Cells were washed with PBS
25 to remove star carboxybetaine polymers. Then, 100 μL of a stock solution containing
26 1 mg/mL of MTT in medium was added and incubated for another 4 h. Then,
27 MTT-containing medium was replaced with 150 μL of DMSO to dissolve the formed
28 crystals at 37 °C for 10 min. The absorbance at a wavelength of 570 nm of each well
29 was measured using a microplate reader. The relative cell viability (%) was
30 determined by comparing the absorbance at 570 nm with control wells.

1

2 **2.10 Blood circulation**

3 All animal experiments were performed according to the guidelines established
4 by the Institute for Experimental Animals of Zhejiang University. Healthy male ICR
5 mice (18–22 g) were purchased from the animal center of Zhejiang Academy of
6 Medical Sciences. The room was maintained at 20 ± 2 °C and $60 \pm 10\%$ relative
7 humidity, with a 12 h light–dark cycle. Mice were fed on water and sterilized food.
8 Prior to treatment, mice were kept fasted overnight. 1 mg of RhB-HEMA labeled
9 polymer in 0.2 mL of PBS was injected via tail vein, and the control group was given
10 only PBS injection. At 2 min, 0.5 h, 2 h, 4 h, 8 h, 12 h, 24 h, 48 h and 96 h, blood
11 samples (50–100 μ l) were collected from orbit. The plasma was separated from the
12 blood by centrifuging at a speed of 4,000 rpm for 5 min. Then, the plasma was diluted
13 with methanol and centrifuged to remove the insoluble solid. The solutions were
14 measured for fluorescent emission at 605 nm with the excitation at 556 nm using a
15 microplate reader (SpectraMax M2e) and the corresponding RhB-HEMA
16 concentration was calculated according to an established standard curve.

17

18 **2.11 Serum-biochemistry evaluation and histopathological examination**

19 For serum-biochemistry evaluation, 1 mg of various RhB-HEMA labeled
20 polymer in 0.2 mL of PBS or 0.2 mL of PBS (control group) were injected via tail
21 vein every two days. After three injections, blood samples were withdrawn from the
22 posterior vena cava under ether anesthesia. HITACHI 7020 automatic analyzer
23 (Hitachi, Tokyo, Japan) was used to measure the total protein (TP), albumin (Alb),
24 globulin (Glo), total bilirubin (TB), bilirubin direct (BD), bilirubin indirect (BI),
25 glutamic-pyruvic transaminase (GPT), glutamic-oxaloacetic transaminase (GOT),
26 alkaline phosphatase (AP), creatinine (Cr), urea nitrogen (UN) and lactate
27 dehydrogenase (LDH). Then, mice were dissected for histopathological examination.
28 A small piece of heart, lung, liver, spleen and kidney were fixed by using 10%
29 formalin and then embedded into paraffin. The section was stained with
30 hematoxylin–eosin (HE) and examined by light microscopy. The data were expressed

1 as mean \pm standard deviation ($n = 5$).

2 **3. Results and Discussion**

3 **3.1 Synthesis and Characterization of Star Carboxybetaine Polymer**

4 A two-step reaction was performed to prepare the desired star carboxybetaine
5 polymer (Scheme 3). First, the β -CD-based macroinitiator was prepared via the
6 reaction of hydroxyl groups on the outside surface of β -CD with 2-bromoisobutyl
7 bromide.²⁶ From ¹H NMR spectroscopy (Figure 1b), a new peak located at $\delta = 1.9$
8 ppm (**a**, C(Br)-CH₃) is observed, which indicates the macroinitiator has been
9 successfully synthesized. The signals located at broad chemical shifts in the region of
10 3.5 - 4.1 ppm are mainly associated with the inner methyldyne and methylene
11 protons between the oxygen and carbon moieties. The peak located at $\delta = 4.6$ ppm is
12 assigned to the inner methyldyne protons between the oxygen moieties (**c**, O-CH-O).
13 From the area ratio of peak **a** to peak **c**, the degree of substitution of the hydroxyl
14 groups on the CD is determined to be about 6.0 (Figure 1b). The star carboxybetaine
15 polymer (CD-CBMA) was subsequently synthesized via ATRP of CBMA from
16 β -CD-based macroinitiator, purified by dialysis against methanol and water to remove
17 unreacted monomers and catalyst (Scheme 3). The CD-CBMAs with different
18 molecular weights were synthesized by varying the feed ratio of monomer to initiator.
19 Table 1 summarizes the GPC results of CD-CBMAs, the number average-molecular
20 weight (Mn) of CD-CBMA increases from 14 kDa to 123 kDa with the increase of
21 feed ratio and the polydispersity index (PDI) of these four CD-CBMAs varies from
22 1.28 to 1.51. These slightly high PDI might be caused by the complex star shape.

23 To evaluate the cell uptake *in vitro* and the pharmacokinetics *in vivo*, CD-CBMA
24 were labeled with fluorescent monomer RhB-HEMA via ATRP. The GPC
25 measurements proved the successful removal of physically adsorbed fluorescent
26 monomer from the RhB-labeled CD-CBMA (Figure 2).

27

28 **3.2 Blood circulation time**

29 To evaluate the *in vivo* stealth property, CD-CBMAs labeled with RhB-HEMA
30 were used for circulation kinetic studies. At various time points, blood was collected

1 to estimate the amount of CD-CBMA remained in bloodstream. Elimination half-life
2 ($t_{1/2}$) and areas under % dose/g versus time curve from 0 to infinity ($AUC_{0 \rightarrow \infty}$) were
3 calculated using two-compartment model and the data are listed in Table 2. As
4 expected, it is found that both $t_{1/2}$ and $AUC_{0 \rightarrow \infty}$ values increase when the molecular
5 weight of these polymers increases from 12 kDa to 123 kDa (Figure 3). The $t_{1/2}$ of
6 CD-CBMA increases dramatically when the molecular weight increases from 12 kDa
7 to 40 kDa. However, further increasing the molecular weight causes a slow increase
8 of $t_{1/2}$. This clear change in $t_{1/2}$ indicates that the threshold MW to avoid rapid renal
9 elimination of CD-CBMA is around 40 kDa, where the hydrodynamic size of
10 CD-CBMA2 is 6.8 nm by DLS, and is a little higher than the pore size of the
11 glomerular membrane of kidney (about 3–5 nm).²⁸ The $t_{1/2}$ for CD-CBMA2 (40 kDa),
12 CD-CBMA3 (58 kDa) and CD-CBMA4 (123 kDa) is 26 h, 36 h and 39 h,
13 respectively. This is a relatively long blood circulating characteristics *in vivo*,
14 especially, molecules at the diameter of the serum protein level (less than 20 nm
15 diameter). This value is comparable to the $t_{1/2}$ of CD-PEGMA300 at similar molecular
16 weight (data not shown). CD-PEGMA300 is poly[poly(ethylene glycol) methyl ether
17 methacrylate] via ATRP from the β -CD initiator for CD-CBMA to make head to head
18 comparison. Jiang and coworkers reported that the circulation half-life of optimized
19 linear pCBMA modified liposome was about 8 h¹⁹, which also suggests the pCBMA
20 could improve the circulation time.

21 Furthermore, the circulation time of repeat injections exhibit similar results to the
22 first injection, implying no immune response occurred (Figure 4). This may be due to
23 the excellent nonfouling properties (<0.3 ng/cm² adsorbed proteins) of zwitterionic
24 polymer on flat surfaces¹⁵ or nanoparticle surfaces²⁹.

25

26 3.3 Serum-biochemistry Evaluation and Histopathological Examination

27 A number of serum-biochemical and histopathological parameters were also
28 compared after three repeat injections of CD-CBMA3 and PBS in order to evaluate *in*
29 *vivo* biocompatibility. Obvious change in such parameters would presumably reflect
30 the occurrence of any abnormality or toxicity in the body. All parameters in the

1 serum-biochemical evaluation, including total protein (TP), total bilirubin (TB),
2 glutamic-pyruvic transaminase (GPT), glutamic-oxaloacetic transaminase (GOT),
3 alkaline phosphatase (AP), creatinine (Cr), urea nitrogen (UN) and lactate
4 dehydrogenase (LDH) were compared. Among them, TB, AP, GPT and GOT levels
5 were attributed to putative functioning of liver; Cr, UN, LDH were attributed to
6 putative functioning of kidney. No significant differences between CD-CBMA3
7 treated mice and PBS treated mice were found (Tables 3). TP, Alb and Glo levels also
8 showed no obvious increase of antibody expression in blood. Moreover, there is few
9 anti-pCBMA antibody observed through a sandwich method detecting the mouse IgG
10 on pCBMA coated gold surface (data not shown). Furthermore, the histopathological
11 evaluation of major organs and tissues including heart, liver, spleen, lung and kidney
12 showed no significant difference with respect to the control (Figure 5), indicating the
13 major organs of mice are still in healthy condition after received three repeated
14 injections of CD-CBMA3. In short, all the results show no clear difference between
15 mice receiving three repeat injections of CD-CBMA3 and the control mice.

16

17 **3.4 *In Vitro* Biocompatibility Analysis of Star Zwitterionic Polymer**

18 The biocompatibility of star zwitterionic polymers was analyzed including
19 plasma compatibility, cell internalization, hemolysis and cell viability. The aims of
20 this study were to investigate *in vitro* behavior to support the unique *in vivo* results.

21

22 **3.4.1 Non-specific Interaction between Star Polymer and Plasma**

23 Non-specific protein adsorption on the blood-contact materials is considered as
24 the first step in foreign-body reaction. High concentration of FBS is one of the most
25 challenging conditions to prevent non-specific protein adsorption on nano drug
26 carriers. The change of particle size measured by DLS provides direct information of
27 hemocompatibility of drug carrier because the adsorption-caused activation or
28 denaturation of serum proteins could cause aggregation, thereby causing the increase
29 of particle size.²⁹ As shown in Figure 6, the size of 5 mg/mL PPO 1 kDa in FBS
30 increased to micrometer level after 1 h, which was attributed to the hydrophobic

1 interaction between PPO and protein in FBS. And there was no large particle detected
2 by DLS after 5 mg/mL CD-CBMA or PEG 2 kDa mixed with FBS. The mixture of
3 CD-CBMA with FBS exhibited almost the same hydrodynamic size as PEG 2 kDa
4 with FBS. No aggregation as PPO 1 kDa was found in either CD-CBMA or PEG 2
5 kDa in FBS. This excellent stability of coexistence of CD-CBMA with FBS indicates
6 very weak non-specific interaction between CD-CBMA with proteins in FBS.

7

8 **3.4.2 Interaction between Star Polymer and Cell Membrane**

9 To evaluate the biocompatibility of CD-CBMAs at cell level, RBC hemolysis
10 assay and macrophage cell uptake were performed. Red blood cell lysis is a widely
11 used method to study polymer–membrane interaction. The observed hemolysis of
12 RBCs in water solutions at 37 °C were used as positive controls, respectively. Figure
13 7 shows that all CD-CBMAs exhibit an undetectable level of hemolytic activity which
14 is comparable with the negative control PEG, while hydrophobic PPO 1 kDa
15 exhibited about 20% hemolytic activity. These phenomenon indicate that the excellent
16 nonfouling nature of zwitterionic polymers could avoid disrupting red blood cell
17 membranes, and CD-CBMAs could be a promising candidate for *in vivo* application,
18 such as systemic drug delivery, through using the hydrophobic cavity of CD to wrap
19 drug molecules and modifying the targeting group with the carboxyl group of CBMA
20 to increase cell uptake.³⁰

21 Furthermore, cell uptake of star polymer CD-CBMA3 (RhB-HEMA labeled) and
22 RhB-HEMA were investigated by fluorescence microscopy and flow cytometry using
23 macrophage RAW 264.7 cell, which is a specialized phagocytic cell that attacks
24 foreign substances, infectious microbes and cancer cells through destruction and
25 ingestion. Even after 12 h incubation with CD-CBMA3, only very weak fluorescence
26 was observed in the cells, whereas strong fluorescence was observed in all cells after
27 12 h incubation with RhB-HEMA at an equivalent concentration of RhB (Figure 8).
28 This result was further confirmed by flow cytometry method quantitatively (Figure 9).
29 After 12 h incubation, the intensity of red fluorescence of RhB from the cells cultured
30 with RhB-HEMA was about 40 times higher than the value obtained from those

1 cultured with RhB-HEMA labeled CD-CBMA3, under condition that an equivalent
2 concentration of RhB was used. These results indicate that the interaction between
3 CD-CBMA and the cell membrane of macrophage cell is very weak due to the
4 superhydrophilic and nonfouling nature of the zwitterionic groups, which is consistent
5 with the result of hemolysis assay.

6

7 **3.4.3 Cell Viability Assay**

8 It is very important to evaluate the potential toxicity of polymer for drug delivery
9 applications. RAW 264.7 and HUVEC cells were used to investigate the cytotoxicity
10 *in vitro*. The cytotoxicity to RAW 264.7 and HUVEC cells in culture medium after 24
11 h incubation with CD-CBMAs was determined using MTT assay. Macrophage cells
12 and endothelial cells were also used because one of the potential uses of these
13 polymers is intravenous drug delivery systems. As shown in Figure 10, even at a
14 concentration up to 2 mg/mL, CD-CBMAs show no obvious cytotoxicity to these two
15 types of cells (> 90% cell viability). The excellent biocompatibility is greatly
16 attributed to the low interaction between polymer and cell membranes, even when
17 cells are growing.

18

19 **4. Conclusion**

20 In this study, star carboxybetaine polymers consisting of a β -CD core and six
21 poly(carboxybetaine) arms were prepared via ATRP from β -CD initiator. *In vivo*
22 experiments showed that this polymer has long-circulation time in mice, even after
23 repeated injections; no appreciable damage or inflammation of major organ tissues,
24 and no obvious increase of antibody occurred in blood. *In vitro* experiments showed
25 that this polymer has reduced internalization, no obvious cytotoxicity and undetectable
26 hemolytic activity, which are consistent with the *in vivo* results. Thus, it is believed
27 that the star carboxybetaine polymer shows great potential for drug delivery systems.

28

29 **Acknowledgments**

30 The authors appreciate financial support from the National Nature Science

1 Foundation of China (21174127, 31350110223), the Ph.D. Programs Foundation of
2 Ministry of Education of China (20110101110034), Zhejiang Provincial Natural
3 Science Foundation of China (LZ13E030001) and the department education of
4 Zhejiang province (Z200804487).

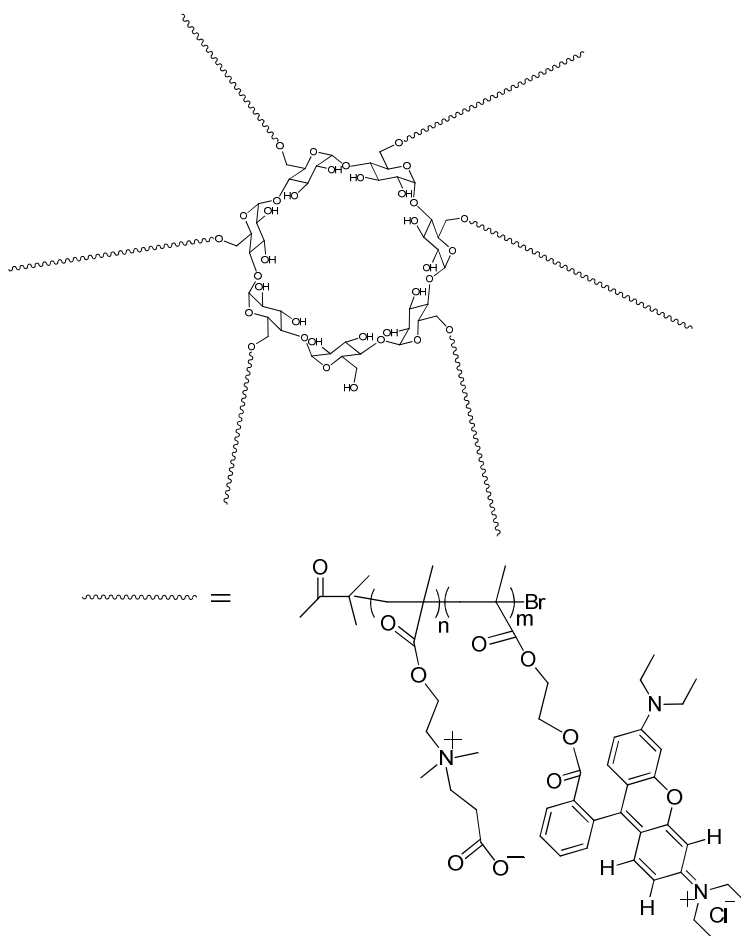
5

6 References

- 7 1. H. Otsuka, Y. Nagasaki and K. Kataoka, *Adv Drug Deliver Rev*, 2003, 55, 403-419.
- 8 2. M. Almgren, W. Brown and S. Hvidt, *Colloid & Polymer Science*, 1995, 273, 2-15.
- 9 3. P. Harder, M. Grunze, R. Dahint, G. M. Whitesides and P. E. Laibinis, *J Phys Chem B*,
10 1998, 102, 426-436.
- 11 4. V. Gaberc-Porekar, I. Zore, B. Podobnik and V. Menart, *Current Opinion in Drug*
12 *Discovery & Development*, 2008, 11, 242-250.
- 13 5. T.-L. Cheng, P.-Y. Wu, M.-F. Wu, J.-W. Chern and S. R. Roffler, *Bioconjugate Chem*,
14 1999, 10, 520-528.
- 15 6. J. Xia, P. L. Dubin and E. Kokufuta, *Macromolecules*, 1993, 26, 6688-6690.
- 16 7. J. Wu, Z. Wang, W. Lin and S. Chen, *Acta Biomaterialia*, 2013, 9, 6414-6420.
- 17 8. K. Ishihara, H. Nomura, T. Mihara, K. Kurita, Y. Iwasaki and N. Nakabayashi, *J Biomed*
18 *Mater Res*, 1998, 39, 323-330.
- 19 9. S. Chen, J. Zheng, L. Li and S. Jiang, *J Am Chem Soc*, 2005, 127, 14473-14478.
- 20 10. R. Matsuno and K. Ishihara, *Nano Today*, 2011, 6, 61-74.
- 21 11. Z. Zhang, T. Chao, S. F. Chen and S. Y. Jiang, *Langmuir*, 2006, 22, 10072-10077.
- 22 12. W. Lin, H. Zhang, J. Wu, Z. Wang, H. Sun, J. Yuan and S. Chen, *J Mater Chem B*, 2013, 1,
23 2482-2488.
- 24 13. G. Z. Li, H. Xue, G. Cheng, S. F. Chen, F. B. Zhang and S. Y. Jiang, *J Phys Chem B*, 2008,
25 112, 15269-15274.
- 26 14. Z. Q. Cao, Q. M. Yu, H. Xue, G. Cheng and S. Y. Jiang, *Angew Chem Int Edit*, 2010, 49,
27 3771-3776.
- 28 15. W. Yang, H. Xue, W. Li, J. L. Zhang and S. Y. Jiang, *Langmuir*, 2009, 25, 11911-11916.
- 29 16. W. Lin, Y. He, J. Zhang, L. Wang, Z. Wang, F. Ji and S. Chen, *Colloids and Surfaces B:*
30 *Biointerfaces*, 2014, 115, 384-390.
- 31 17. S. F. Chen, L. Y. Li, C. Zhao and J. Zheng, *Polymer*, 2010, 51, 5283-5293.
- 32 18. S. F. Chen, Z. Q. Cao and S. Y. Jiang, *Biomaterials*, 2009, 30, 5892-5896.
- 33 19. W. Lin, J. Zhang, Z. Wang and S. Chen, *Acta Biomaterialia*, 2011, 7, 2053-2059.
- 34 20. Z. Cao and S. Jiang, *Nano Today*, 2012, 7, 404-413.
- 35 21. W. Yang, S. Liu, T. Bai, A. J. Keefe, L. Zhang, J.-R. Ella-Menye, Y. Li and S. Jiang, *Nano*
36 *Today*, 2014, 9, 10-16.
- 37 22. Z. Q. Cao, L. Zhang and S. Y. Jiang, *Langmuir*, 2012, 28, 11625-11632.
- 38 23. M. Elsbahy, A. Li, F. Zhang, D. Sultan, Y. Liu and K. L. Wooley, *J Control Release*,
39 2013.
- 40 24. L. Qiu and Y. Bae, *Pharmaceut Res*, 2006, 23, 1-30.
- 41 25. T. D. McCarthy, P. Karellas, S. A. Henderson, M. Giannis, D. F. O'Keefe, G. Heery, J. R.
42 A. Paull, B. R. Matthews and G. Holan, *Molecular Pharmaceutics*, 2005, 2, 312-318.

- 1 26. F. J. Xu, Z. X. Zhang, Y. Ping, J. Li, E. T. Kang and K. G. Neoh, *Biomacromolecules*,
2 2009, 10, 285-293.
- 3 27. M. A. Dobrovolskaia, J. D. Clogston, B. W. Neun, J. B. Hall, A. K. Patri and S. E. McNeil,
4 *Nano Letters*, 2008, 8, 2180-2187.
- 5 28. P. Caliceti and F. M. Veronese, *Adv Drug Deliver Rev*, 2003, 55, 1261-1277.
- 6 29. W. Yang, L. Zhang, S. L. Wang, A. D. White and S. Y. Jiang, *Biomaterials*, 2009, 30,
7 5617-5621.
- 8 30. S. Jiang and Z. Cao, *Adv Mater*, 2010, 22, 920-932.
- 9
10

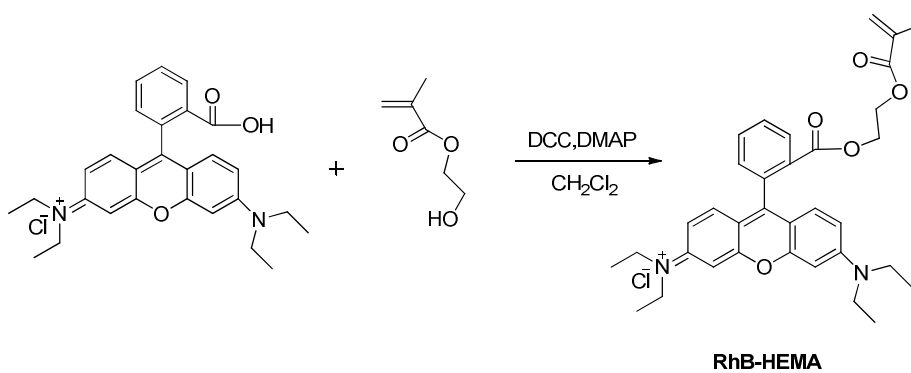
1



2

3 Scheme 1. Chemical structure of star carboxybetaine polymer.

4

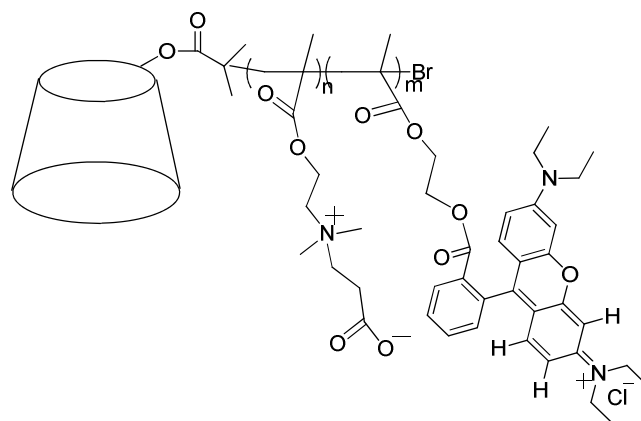
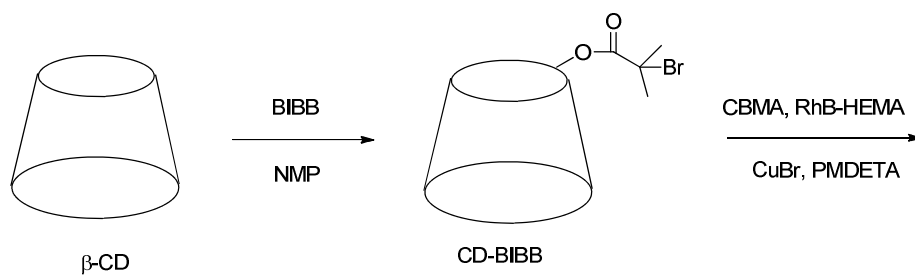


5

6 Scheme 2. Synthesis procedure of rhodamine B-based fluorescent monomer
7 (RhB-HEMA).

8

9



CD-CBMA(RhB labeled)

1
 2 Scheme 3. Synthesis procedure of macroinitiator CD-BIBB and RhB-labeled star
 3 polymer CD-CBMA.

4

5

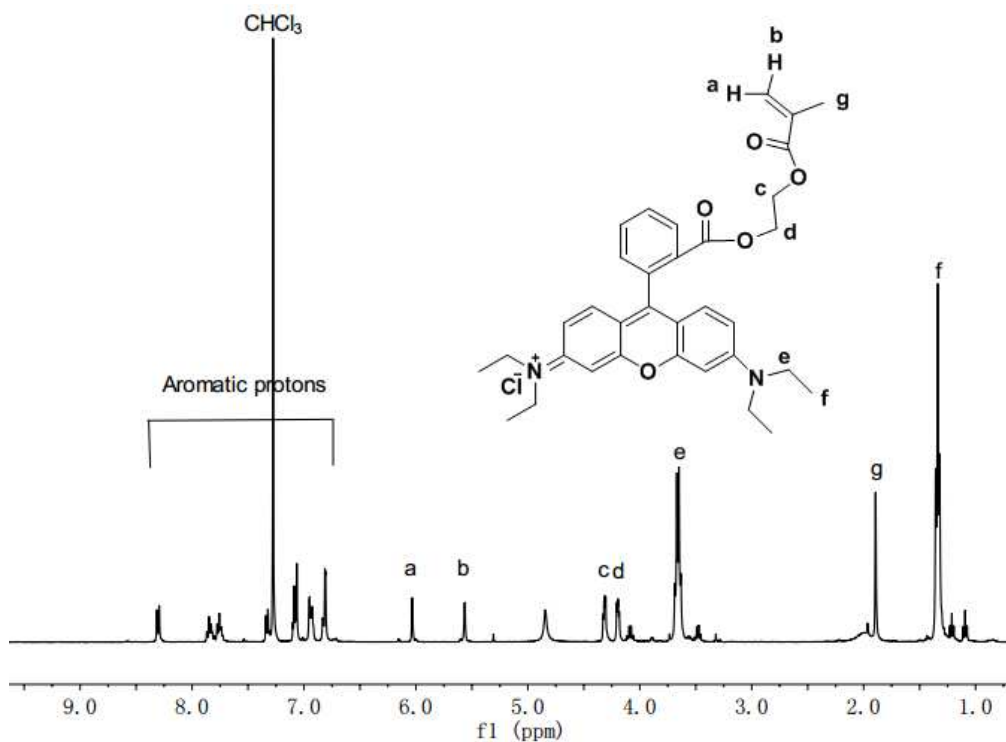
6

7

8

9

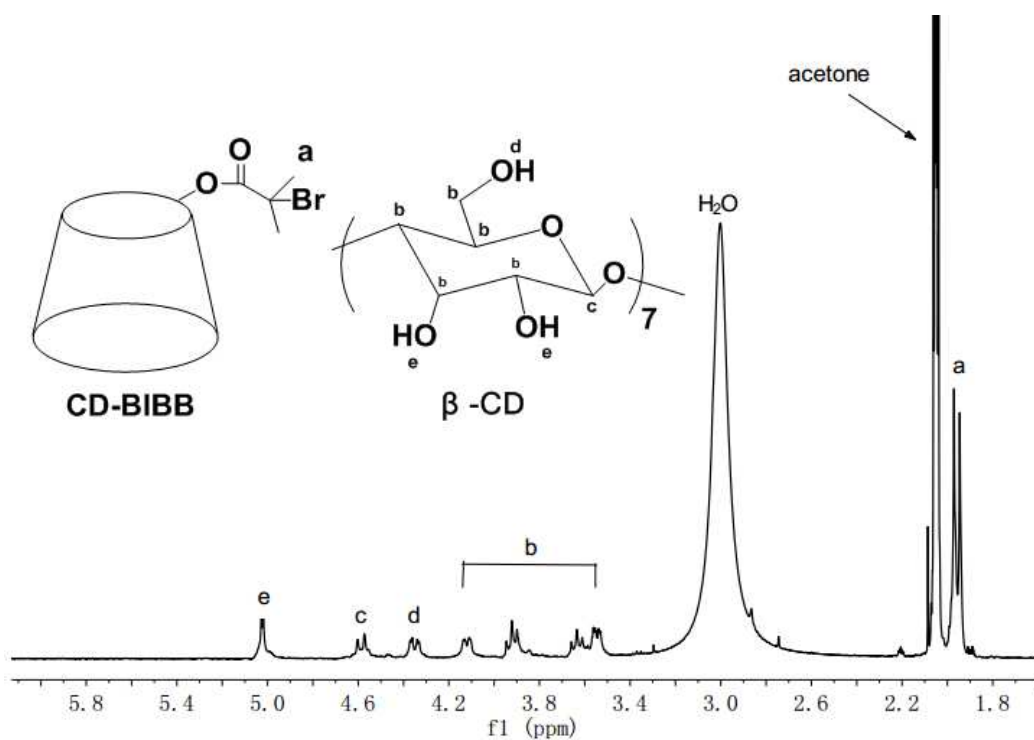
10



1

2

(a)



3

4

(b)

5 Figure 1. ^1H NMR spectra of (a) RhB-HEMA in CDCl_3 ; (b) Macroinitiator CD-BIBB
6 in acetone- D_6 .

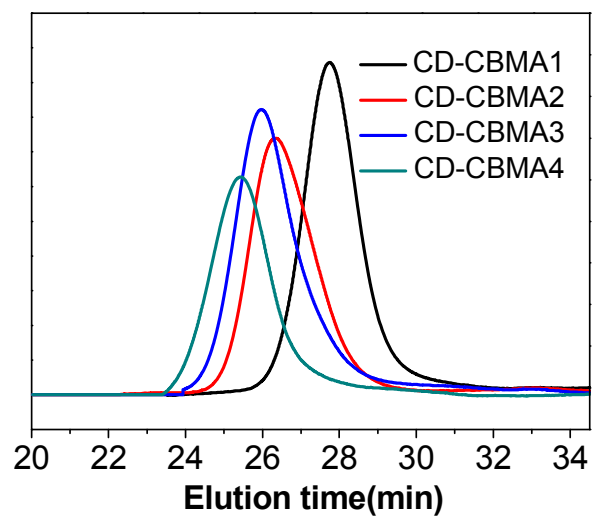
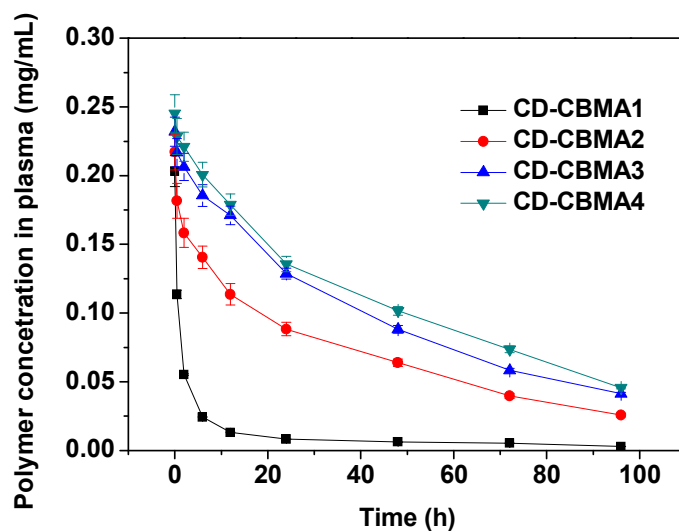


Figure 2. GPC traces of star polymer CD-CBMA.

1
2
3
4
5
6
7
8
9
10
11
12



1

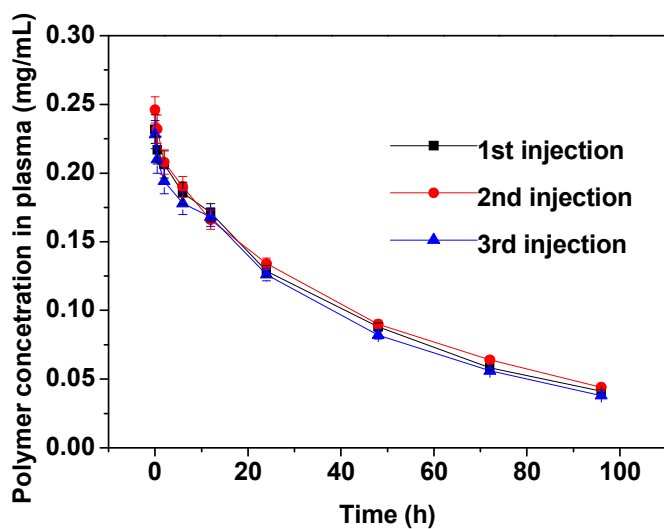
2 Figure 3. Polymer concentration in plasma with respect to time after intravenous
3 administration (mean \pm SD, $n = 3$).

4

5

6

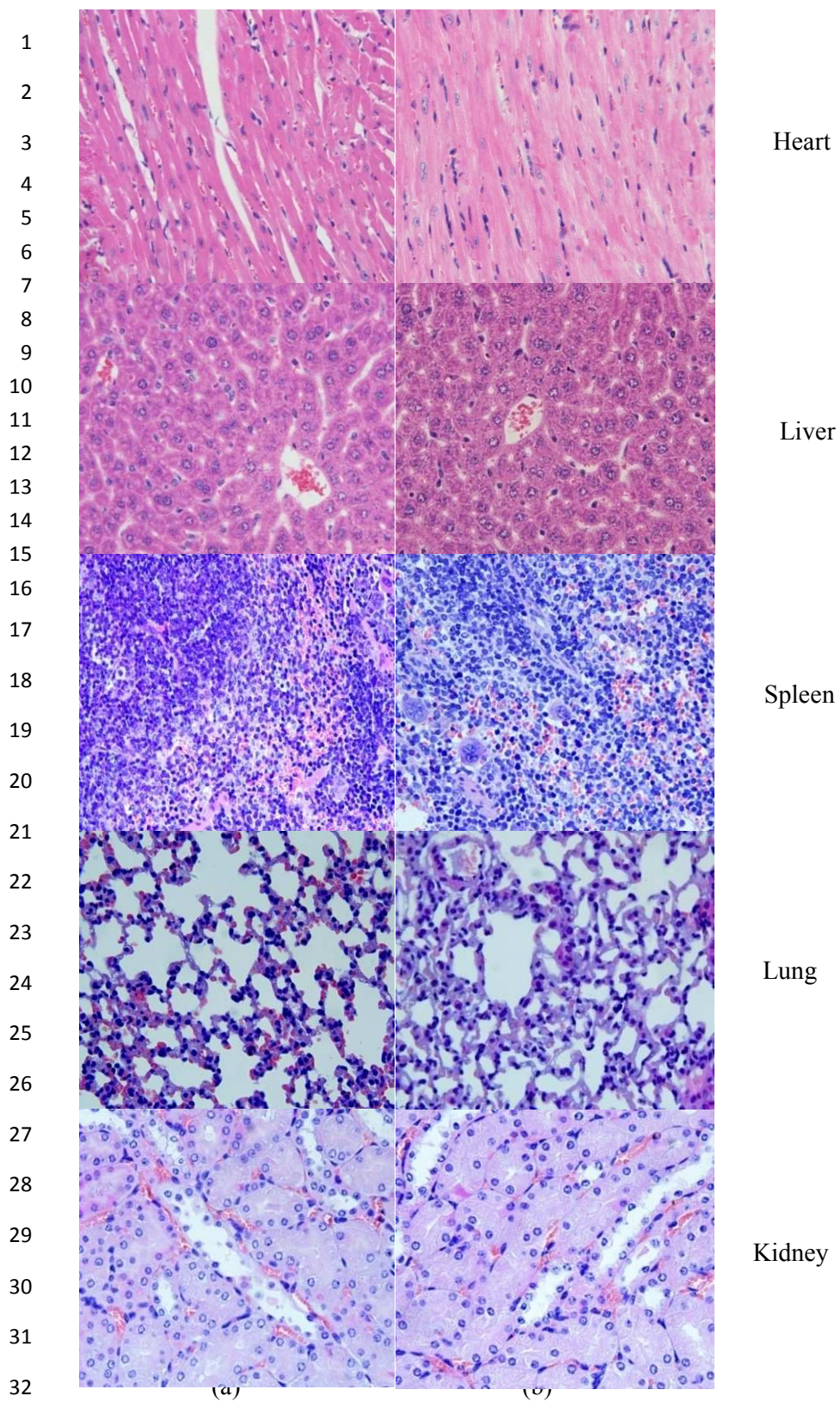
7



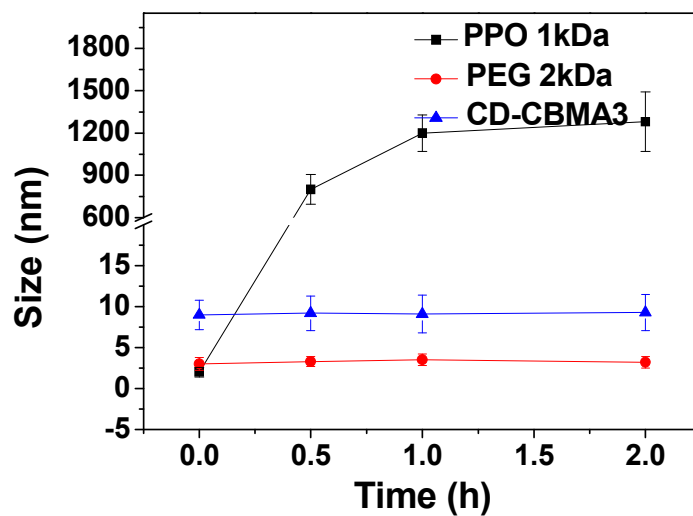
8

9 Figure 4. CD-CBMA3 concentration in plasma with respect to time after intravenous
10 administration (mean \pm SD, $n = 3$).

11

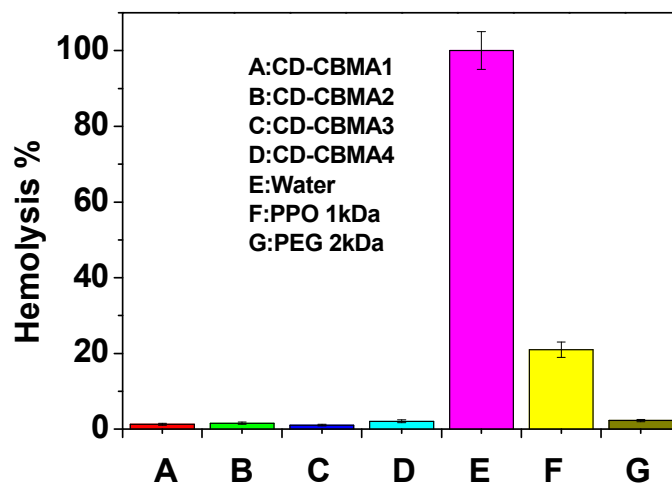


33 Figure 5. Histopathology of heart, liver, spleen, lung, kidney after (a) PBS and (b)
34 CD-CBMA3 treatment.

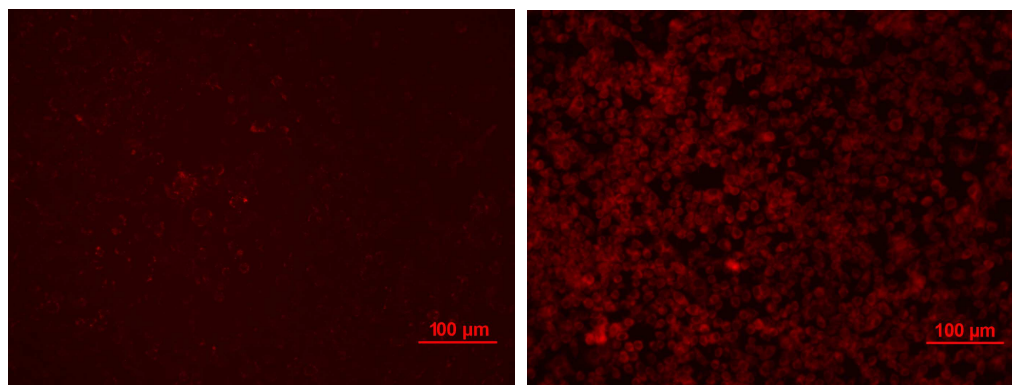


1
2 Figure 6. Size of CD-CBMA3, PPO 1 kDa and PEG 2 kDa versus time in FBS at
3 37 °C.

4
5
6
7



8
9 Figure 7. Hemolysis assay of star polymer CD-CBMA, PPO 1 kDa and PEG 2 kDa
10 with different molecular weights (mean \pm SD, $n = 3$).



1

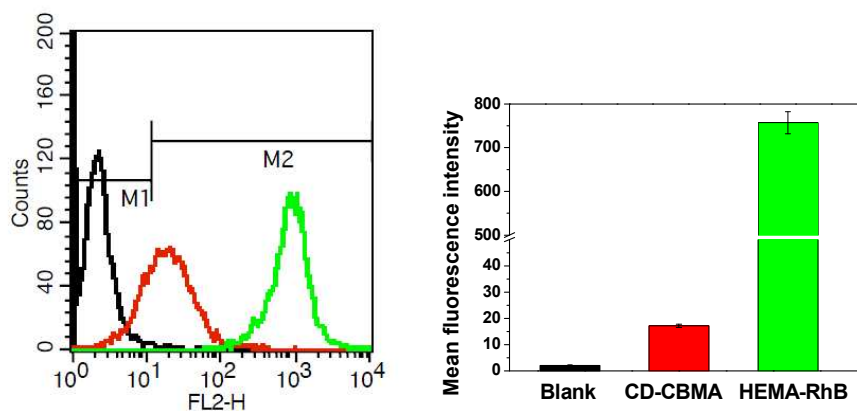
2

(a)

(b)

3 Figure 8. Cell uptake of star polymer CD-CBMA3 (RhB-HEMA labeled) and
 4 RhB-HEMA followed by fluorescence microscopy using macrophage RAW 264.7
 5 cells. (a) After 12 h incubation with CD-CBMA (exposure time is 3 s); (b) After 12 h
 6 incubation with RhB-HEMA (exposure time is 0.2 s).

7



8

9

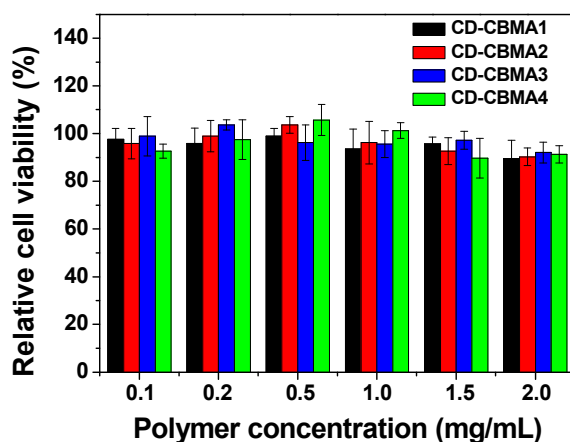
(a)

(b)

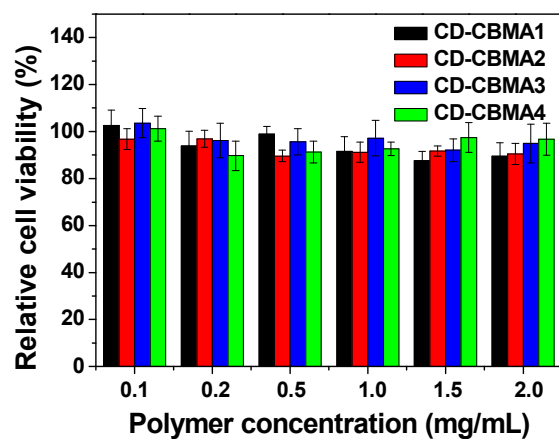
10 Figure 9. (a) Flow cytometry results of RAW 264.7 cells treated by PBS (black),
 11 CD-CBMA (RhB-HEMA labeled) (red), free RhB-HEMA (green) at 37 °C for 12 h;
 12 (b) Mean fluorescence intensity located in the RAW 264.7 cells incubated in PBS,
 13 CD-CBMA(RhB-HEMA labeled) and free RhB-HEMA at 37 °C for 12 h.
 14 RhB-HEMA concentration was 2 μg/ml.

15

16



(a)



(b)

Figure 10. Cytotoxic of star polymer CD-CBMA at polymer concentrations ranging from 0.1 mg/mL to 2 mg/mL after 24 h incubation with cells. Relative cell viability are shown as mean \pm SD, $n = 4$. (a) RAW 264.7 cells, (b) HUVEC cells.

1 Table 1. Feed molar ratio of monomer to initiator, number-average molecular weights
 2 (Mn), polydispersity index (PDI) and size for star polymer CD-CBMA.

Sample	[CBMA]:[CD-BIBB] ^a	Mn (kDa) ^b	PDI ^b	Size (nm) ^c
CD-CBMA1	120	14	1.28	3.0 ± 0.4
CD-CBMA2	300	40	1.34	6.8 ± 0.8
CD-CBMA3	600	58	1.31	8.7 ± 2.6
CD-CBMA4	1200	123	1.51	11.9 ± 2.5

3 ^aReaction molar ratios of CBMA monomer to CD-BIBB initiator used.

4 ^bDetermined by GPC.

5 ^cEstimated by DLS.

6

7 Table 2. $T_{1/2}$ and $AUC_{0-\infty}$ determined from pharmacokinetic analysis for the Evaluated Polymers.

Sample	$t_{1/2}$ (h)	$AUC_{0-\infty}$ (mg/mL/h)
CD-CBMA1	0.92 ± 0.08	0.26 ± 0.04
CD-CBMA2	26.6 ± 2.3	6.97 ± 0.71
CD-CBMA3	36.0 ± 3.1	11.3 ± 1.7
CD-CBMA4	39.1 ± 3.7	13.0 ± 1.5

8

9

10

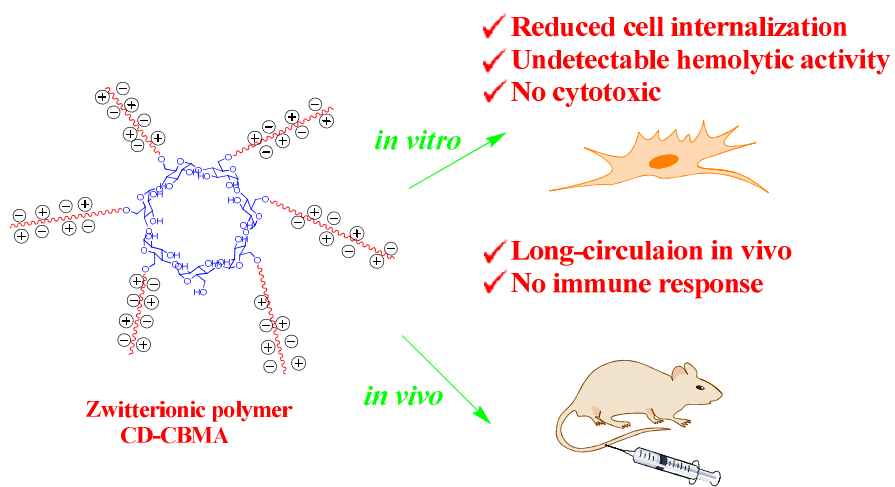
1 Table 3. Blood test parameters for mice treated with PBS and CD-CBMA (mean \pm SD, $n = 3$).

Materials	PBS	CD-CBMA3
Total Protein(g/L)	50.9 \pm 0.5	49.2 \pm 0.6
Albumin (g/L)	32.6 \pm 0.2	31.1 \pm 0.3
Globulin (g/L)	18.3 \pm 0.3	18.1 \pm 0.3
Total Bilirubin(umol/L)	5.8 \pm 0.2	5.0 \pm 0.2
Bilirubin Direct(umol/L)	2.6 \pm 0.2	2.0 \pm 0.2
Bilirubin Indirect(umol/L)	3.2 \pm 0.1	3.3 \pm 0.2
Glutamic-Pyruvic Transaminase(U/L)	19 \pm 4	24 \pm 2
Glutamic-Oxaloacetic Transaminase(U/L)	75 \pm 6	74 \pm 8
Alkaline Phosphatase(U/L)	101 \pm 8	97 \pm 4
Creatinine(umol/L)	42.7 \pm 1.8	36.7 \pm 1.3
Urea Nitrogen(umol/L)	8.3 \pm 0.4	8.8 \pm 0.2
Lactate Dehydrogenase(U/L)	593 \pm 60	618 \pm 67

2

3

1 Graphical Abstrate



2